PARTICLE IMPACT DAMPING:

INFLUENCE OF MATERIAL AND SIZE

A Thesis

by

KUN SAPTOHARTYADI MARHADI

Submitted to the Office of Graduate Studies of
Texas A&M University
in partial fulfillment of the requirements for the degree of

MASTER OF SCIENCE

December 2003

Major Subject: Aerospace Engineering

PARTICLE IMPACT DAMPING:

INFLUENCE OF MATERIAL AND SIZE

A Thesis

by

KUN SAPTOHARTYADI MARHADI

Submitted to Texas A&M University
in partial fulfillment of the requirements
for the degree of

MASTER OF SCIENCE

Approved as to style and content by:

Vikram K. Kinra (Chair of Committee)	Thomas W. Strganac (Member)
Luis A. San Andres (Member)	Walter E. Haisler (Interim Head of Department)

December 2003

Major Subject: Aerospace Engineering

ABSTRACT

Particle Impact Damping: Influence of Material and Size.

(December 2003)

Kun Saptohartyadi Marhadi, B.S., Texas A&M University

Chair of Advisory Committee: Dr. Vikram K. Kinra

In this study, particle impact damping is measured for a cantilever beam with a particle-filled enclosure attached to its free end. Many particle materials are tested: lead spheres, steel spheres, glass spheres, tungsten carbide pellets, lead dust, steel dust, and sand. The effects of particle size are also investigated. Particle diameters are varied from about 0.2 mm to 3 mm. The experimental data collected is offered as a resourceful database for future development of an analytical model of particle impact damping.

For my parents, for their continuous love and compassion.

ACKNOWLEDGEMENTS

First of all, I would like to thank Allah, God the Almighty, the Most Merciful and the Most Compassionate. It is because of Him alone that I am able to complete my study. I wish to thank Dr. Vikram Kinra, my advisor, for his motivation and guidance during my graduate study. I wish to thank Dr. Thomas Strganac for his keen and ongoing interest in the development of my thesis. I wish to thank Dr. Luis San Andres for serving on my committee. I would like to thank all the professors in the Aerospace Engineering Department, especially Dr. Haisler, for passing their knowledge on to me.

This thesis has been substantially modified from the original thesis reviewed and presented at the thesis defense. Several key questions concerning the experimental results arose during the defense. With the support of my major advisor, further research was performed in order to obtain satisfactory explanation of those questions. During this effort, it was discovered that the primary equipment used (laser vibrometer) could not properly obtain measurements required at low frequencies, and the results were shifted by an unknown bias. It was further determined that the equipment would require re-calibration, if feasible, at the manufacturer's site. Hence, it was decided to present this thesis as a continuation of the work by Friend and Kinra (see reference [8]) as originally planned, but focus the attention on providing the experimental results as a set of viable measurements that are of reasonable quality for future study.

NOMENCLATURE

d	clearance of the enclosure
g	acceleration of gravity = 9.81 m/s^2
m	mass of the particles
M	primary mass
R	effective coefficient of restitution
T	maximum kinetic energy during a cycle
ΔT	kinetic energy dissipated during a cycle
U	displacement amplitude of the primary mass
V	velocity amplitude of the primary mass
v_p	velocity of the particle
Δ	dimensionless clearance
Γ	dimensionless acceleration amplitude
μ	mass ratio
ω	undamped circular natural frequency
Ψ	specific damping capacity

TABLE OF CONTENTS

Page

ABSTRACT iii

DEDICATION. iv

ACKNOWLEDGEMENTS v

NOMENCLATURE vi

TABLE OF CONTENTS vii

LIST OF FIGURES viii

LIST OF TABLES ix

1. INTRODUCTION 1

2. THEORETICAL ANALYSIS 4

3. EXPERIMENTAL PROCEDURES 7

4. EXPERIMENTAL RESULTS 10

4.1 Damping due to Particles 10
4.2 The Effects of Particle Materials on Damping 14
4.3 The Effects of Number of Particles 18
4.4 The Effects of Particle Size 21
4.5 Dust Like Particles 24

5. CONCLUSION 26

REFERENCES 27

VITA 28

LIST OF FIGURES

Page

Figure 1. Enclosure with an adjustable clearance and the experimental setup. 9

Figure 2. A comparison of typical experimental velocity waveforms with and without particles. 1.2 mm lead spheres, $\mu = 0.1$ and $\Delta = 5.65$. Frequency = 16 Hz. 11

Figure 3. Kinetic energy dissipated per cycle versus velocity amplitude. 1.2 mm lead spheres, $\mu = 0.1$ and $\Delta = 5.65$. 12

Figure 4. Specific damping capacity of beam with particles versus dimensionless acceleration amplitude. 1.2 mm lead spheres and $\Delta = 5.65$. 13

Figure 5. Comparison of different particle materials for the same mass ratio. $\mu = 0.06$ (a) $\Delta = 1.13$; (b) $\Delta = 2.26$; 15

Figure 6. Comparison of different materials for the same size, shape, and number of particles. $\Delta = 5.65$. (a) 1 layer. 207 Particles; 19

Figure 7. Comparison of different particle sizes for the same mass ratio. Glass spheres. $\mu = 0.02$. $\Delta = 5.65$. 22

Figure 8. Comparison of different particle sizes and number of particles. Glass spheres. $\Delta = 5.65$. 23

Figure 9. Experimental results of dust like particles. $\mu = 0.06$. $\Delta = 5.25$. 25

LIST OF TABLES

Page

Table 1. Particles tested, for $\mu = 0.06$ 14

Table 2. Dust like particles tested, for $\mu = 0.06$ 24

1. INTRODUCTION

Particle impact damping (PID) is a method to increase structural damping by inserting particles in an enclosure attached to a vibrating structure. The particles absorb kinetic energy of the structure and convert it into heat through inelastic collisions between the particles and the enclosure. Additional energy dissipation may also occur due to frictional losses and inelastic particle-to-particle collisions amongst the particles. The unique aspect of PID is that high damping is achieved by converting kinetic energy of the structure to heat as opposed to the more traditional methods of damping where the elastic strain energy stored in the structure is converted to heat.

Viscoelastic materials have wide applications in vibration damping in a normal environment, i.e. under ambient temperature and pressure. However, they lose their effectiveness in very low and high temperature environments and degrade over time. Particle impact damping offers the potential for the design of a better passive damping technique with minimal impact on the strength, stiffness and weight of a vibrating structure. With a proper choice of particle material, this technique appears to be independent of temperature and is very durable.

Earlier studies have investigated the energy loss mechanisms and characteristic of particle impact dampers under various excitation models. Saluena *et al*. [1] have studied mathematically the dissipative properties of granular materials using particle dynamic method. They showed how the analysis of energy-loss rate displays different damping regimes in the amplitude-frequency plane of the excitation force. Tianning *et al*. [2] performed numerical modeling of particle damping with discrete element method.

This thesis follows the style and format of *Journal of Sound and Vibration*.

They showed that under different vibration and particle system parameters, the collision and friction mechanism might play different or equivalent roles in energy dissipation.

Some experimental studies have also been conducted to measure particle impact damping at low frequencies (below 20 Hz). Papalou and Masri [3] studied the behavior of particle impact dampers in a horizontally vibrating single degree of freedom (SDOF) system under random base excitation. Using tungsten powder, they studied the influence of mass ratio, container dimensions, and excitation levels. They provided optimum design of particle damper based upon reduction in system response. Cempel and Lotz [4] used a simplified energy approach to measure the influence of various particle-packing configurations on the damping loss factor of a SDOF system under horizontal forced vibration. Popplewell and Semercigil [5] conducted experiments to study the performance of a plastic "bean bag" filled with lead shot in reducing vibration. They observed that a plastic bean bag not only exhibited a greater damping effectiveness but also "softer" impacts than a single lead slug of equal mass.

Panossian [6, 7] conducted a study of non-obstructive particle damping in the modal analysis of structures at a higher frequency range of 300 Hz to 5,000 Hz. This method consists of drilling small diameter cavities at appropriate locations in a structure and partially or fully filling the holes with particles of different materials and sizes (steel shot, tungsten powder, nickel powder, etc.). Significant decrease in structural vibrations was observed even when the holes were completely filled with particles and subjected to a pressure as high as 240 atmosphere.

Friend and Kinra [8] conducted a study of particle impact damping in the context of free decay of a cantilever beam in the vertical plane. In their study, PID was measured

for a cantilever beam with the enclosure attached to its free end. Lead powder was used throughout the study. They studied the effects of vibration amplitude and particle fill ratio (or clearance) on damping. PID was observed to be highly nonlinear, i.e. amplitude dependent. A very high value of maximum specific damping capacity (50%) was achieved in the experiment. An elementary analytical model was also constructed to capture the essential physics of particle impact damping. A satisfactory agreement between the theory and experiment was observed.

This work is a continuation of the work by Friend and Kinra [8]. The primary objective of this work is to expand the previous experiments in order to collect PID characteristics of various particle materials and particle sizes. Using the same method and experimental procedures developed by Friend and Kinra, experiments are conducted for lead spheres, steel spheres, glass spheres, sand, steel dust, lead dust, and tungsten carbide pellets. The particle diameter varies from about 0.2 mm to 3 mm. Tests are conducted for different vibration amplitudes, clearances, and number of particles.

2. THEORETICAL ANALYSIS

In the following, a summary of the theory developed by Friend and Kinra [8] that pertains to experiments in this study is presented. We assume that the reader has already read the work by Friend and Kinra. The theory begins with the idealization of the beam as a standard Euler-Bernoulli beam and the enclosure as a point mass attached to the tip of the beam. The continuous beam is then reduced to an equivalent single degree of freedom system. The reduced mass of the beam, M is referred to the primary mass of the equivalent single degree of freedom system. For the beam used in this study, M is equal to 0.24 of the total mass of the beam plus the mass of the enclosure.

Specific damping capacity, Ψ, is defined as the kinetic energy converted into heat per cycle (ΔT) normalized with respect to the maximum kinetic energy of the structure per cycle (T), i.e.

$$\Psi=\Delta T/T. \tag{1}$$

A cycle is defined as the duration between two successive peaks in the velocity of the primary mass, V. Then, T is maximum at the start of a cycle and is given by

$$T=\frac{1}{2}MV^2. \tag{2}$$

The energy dissipated during the i^{th} cycle is calculated using

$$\Delta T_i = T_i - T_{i+1}. \tag{3}$$

In reality, there are times during a cycle when particles move separately from the enclosure, and some other times they move in contact with the enclosure. Since our method of experiment cannot determine whether or not the particles in contact with the enclosure at any given instant, we assume that the particles are always in contact with the

enclosure at velocity peaks. Then, the primary mass, *M*, includes the mass of the particles, *m*, and the energy dissipated can be expressed as

$$\Delta T_i = \frac{1}{2} M \left(V_i^2 - V_{i+1}^2 \right). \tag{4}$$

Substituting equations (4) and (2) into equation (1), we express damping during the i^{th} cycle as

$$\Psi_i = \frac{V_i^2 - V_{i+1}^2}{V_i^2}. \tag{5}$$

Friend and Kinra introduced a parameter *R* (effective coefficient of restitution) that will give the measure of how much energy dissipation occurs due to inelastic collisions and frictional sliding amongst the particles, and between the particles and the enclosure walls. Defining $v_p^-(v_p^+)$ and $v_2^-(v_2^+)$ be respectively the velocities of the particle and the primary mass before (after) the impact, they defined *R* as

$$R = -\frac{(v_p^+ - v_2^+)}{(v_p^- - v_2^-)} \qquad 0 \le R \le 1. \tag{6}$$

then, the energy dissipated during an impact may be expressed as

$$\Delta T = \frac{1}{2}(1 - R^2) \frac{m}{1 + \mu} \left(v_p^- - v_2^- \right)^2, \tag{7}$$

where μ is the mass ratio of the particles with respect to the primary mass, *m*/*M*. *R* is estimated by minimizing the difference between theory and experiment using least square method.

There are several parameters that affect energy dissipation during an impact, i.e.

$$\Delta T = f(m, d, g, M, \omega, U; R), \tag{8}$$

where g is the gravitational constant, ω is the fundamental frequency (radians/second), d is the clearance, which is the distance between the top of the bed of particles at rest and the ceiling of the enclosure, and U is the amplitude. The semicolon separating R is used to emphasize that R is obtained by curve fitting experimental data to the model. In dimensionless parameters, the damping can be seen as:

$$\Psi = f(\mu, \Delta, \Gamma; R), \tag{9}$$

where

$\Delta \equiv \frac{d\omega^2}{g}$ = dimensionless clearance, and

$\Gamma = \frac{U\omega^2}{g}$ = dimensionless acceleration amplitude, in units of g.

In this study, dimensionless parameters will be extensively used to present all experimental results.

3. EXPERIMENTAL PROCEDURES

A schematic of the test setup is shown in Figure 1. The experimental setup consists of a particle enclosure attached to a steel beam that is made of 4140 steel (Young's modulus, E = 207 Gpa and density = 7.84×10^3 kg/m^3), and which is clamped in a vise grip. The clearance, d, can be varied by adjusting the ceiling of the enclosure using a threaded screw. The particles are contained within a cylindrical plexiglas wall, and the floor and ceiling are made of aluminum. The mass of the enclosure is 67.1 grams, and its interior dimensions are: diameter = 19.1 mm and maximum height = 25.4 mm. The cantilever beam dimensions are: length = 306.6 mm, width = 19.16 mm, and height = 3.16 mm. The mass of the beam is 145.5 grams. The natural frequency of the fundamental mode of the beam with the enclosure attached was found to be 16.7 Hz. The intrinsic material damping of the beam was measured to be about 1%.

A coil connected to a DC power supply is used to provide a constant magnetic force to a steel plate mounted to the bottom of the enclosure. The vertical position of the coil is adjusted to provide an initial displacement, U_o. At time $t = 0$, the current to the coil is switched off, and the beam is allowed to decay freely.

An OFV300 Polytec laser vibrometer is used to measure velocity of the enclosure. A piece of lightweight retroreflecting tape is attached to the top center of the enclosure for reflecting the incident laser beam. The velocity is measured to a resolution of 1 μm/s. In our experiments, the velocity amplitude ranges from 30 mm/s to 2,000 mm/s. Consequently, the signal-to-noise ratio varies from 3×10^4 to 2×10^6, which is very high.

Data acquisition is triggered at $t = 0$, and the decaying waveform is collected with a Yokogawa DL708 Digital Processing Oscilloscope (DPO). The DPO has a 16-bit

vertical resolution (1 part per 65,536), a maximum digitizing rate of 10^5 points/s (i.e. a 10 μs interval) and a maximum record length of 4×10^6 points. During experiments, the digitizing rate is set at 2,000 points/s. For a nominal frequency of 16 Hz observed in this study, this translates to 125 points/cycle.

In this study, seven different particle materials are tested. These particles, followed by their diameters are the following: lead spheres (1.2 mm), steel spheres (1.17 mm), glass spheres (0.5, 1.12, and 3 mm), irregular tungsten carbide pellets (equivalent diameter 0.5 mm), sand (equivalent diameter 0.2 mm), steel powder (equivalent diameter 0.5 mm), and lead dust (equivalent diameter 0.2 mm). Each type of particles is tested with a mass of 6.5 grams, which corresponds to $\mu = 0.06$. Tests are conducted with $\Delta = 1.13$, 2.26, 3.36, 4.52, 5.25, 5.65, or 7.91, and $1 \leq \Gamma \leq 10$. For each clearance, tests are repeated 8 times with different initial amplitudes. Damping for each cycle, Ψ_i, is determined using equation (5).

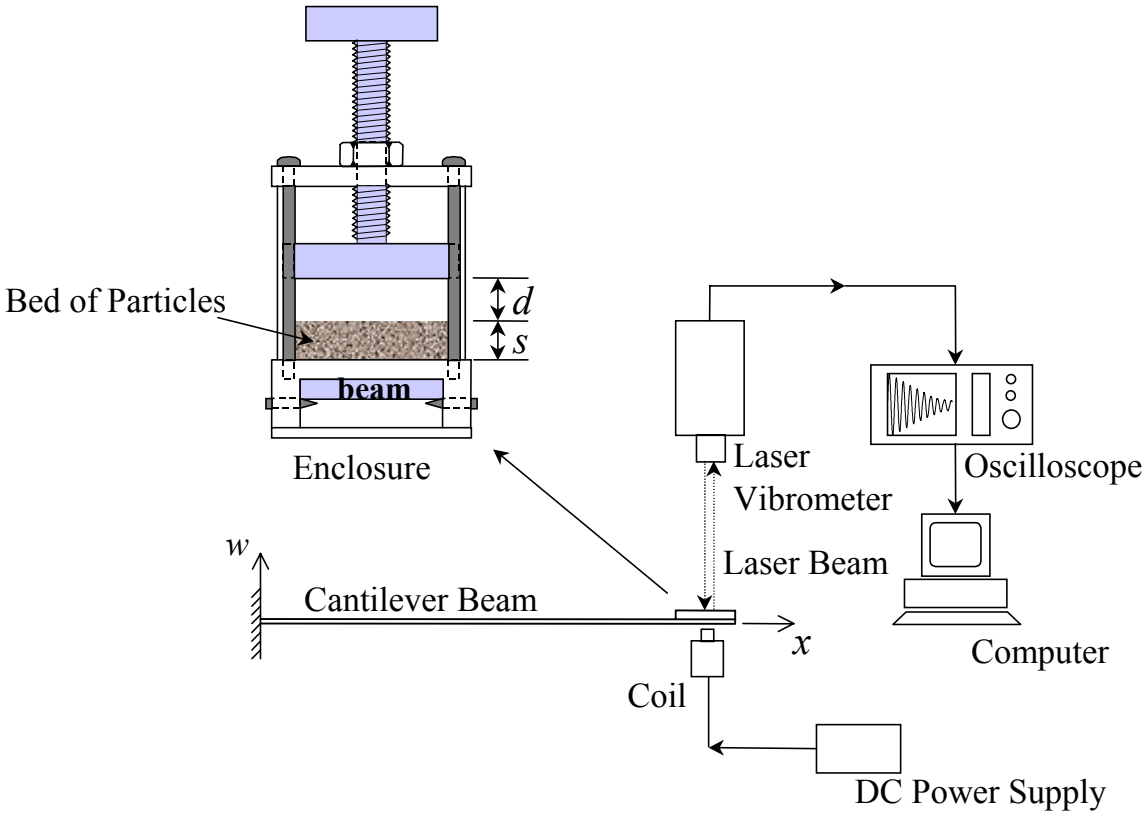

Figure 1. Enclosure with an adjustable clearance and the experimental setup.

4. EXPERIMENTAL RESULTS

4.1 Damping due to Particles

Figure 2 shows a typical waveform comparison of the beam with and without particles. The particles used were 1.2 mm diameter lead spheres with $\mu = 0.1$ and $\Delta = 5.65$. It is clear that the presence of the particles causes a significant decrease in velocity after a few cycles. In Figure 3, the kinetic energy dissipated per cycle is presented as a function of maximum velocity at the beginning of each cycle, along with the maximum kinetic energy in the cycle. The experimental results presented here are a compilation of 8 individual tests, each with different starting point.

The damping, Ψ, is presented in Figure 4 as a function of dimensionless acceleration amplitude, Γ. The dash line in the figure shows the location of $\Gamma_{critical}$, at which the particles first osculate with the ceiling according to [8]. Damping for other values of μ is also plotted in the same figure. As expected, damping increases with mass ratio. For $\mu = 0.1$, the damping can reach as high as 45%. For $\mu = 0.04$ and 0.02 the damping can reach 21% and 12% respectively. Hence, damping can be achieved one order of magnitude higher than the intrinsic material damping of the steel beam with a small additional weight of particles.

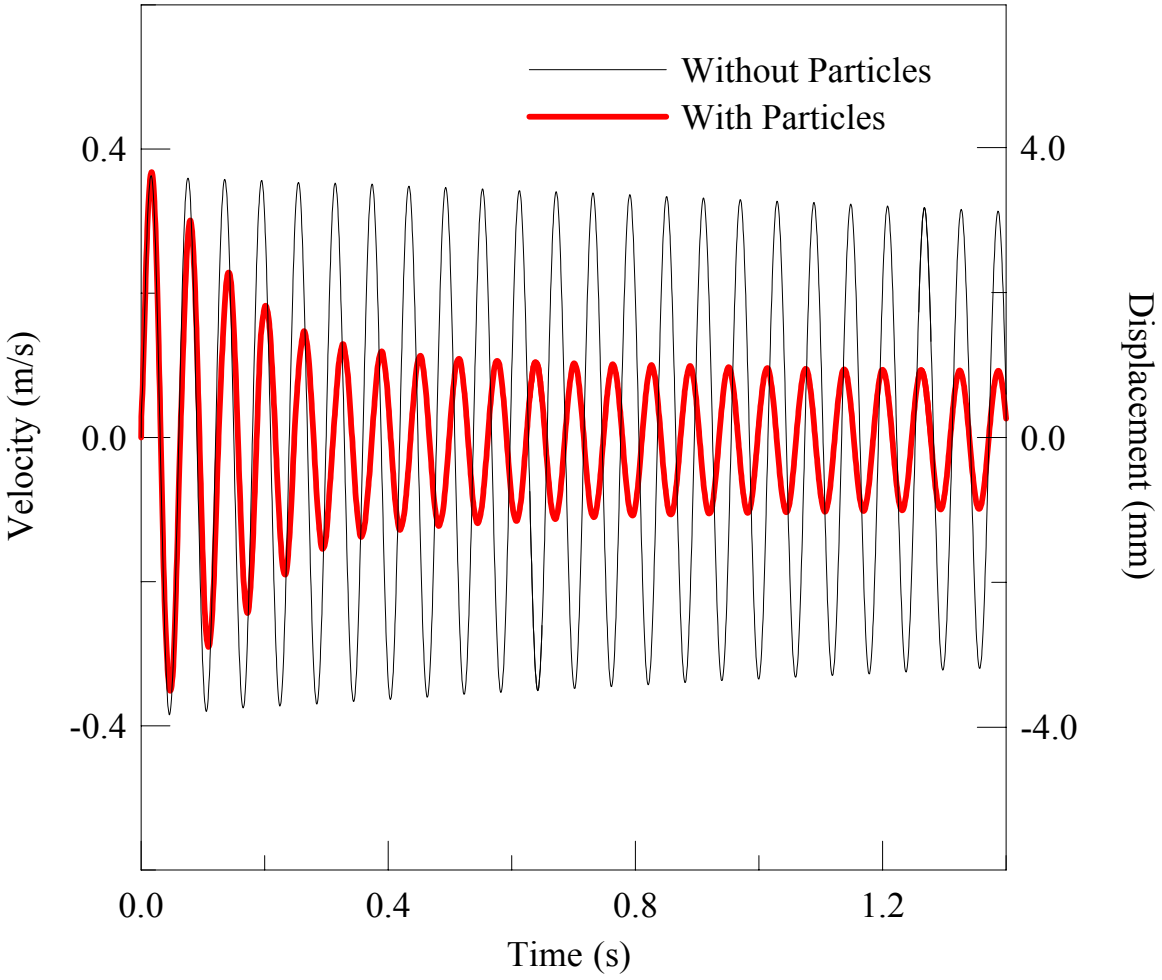

Figure 2. A comparison of typical experimental velocity waveforms with and without particles. 1.2 mm lead spheres, $\mu = 0.1$ and $\Delta = 5.65$. Frequency = 16 Hz.

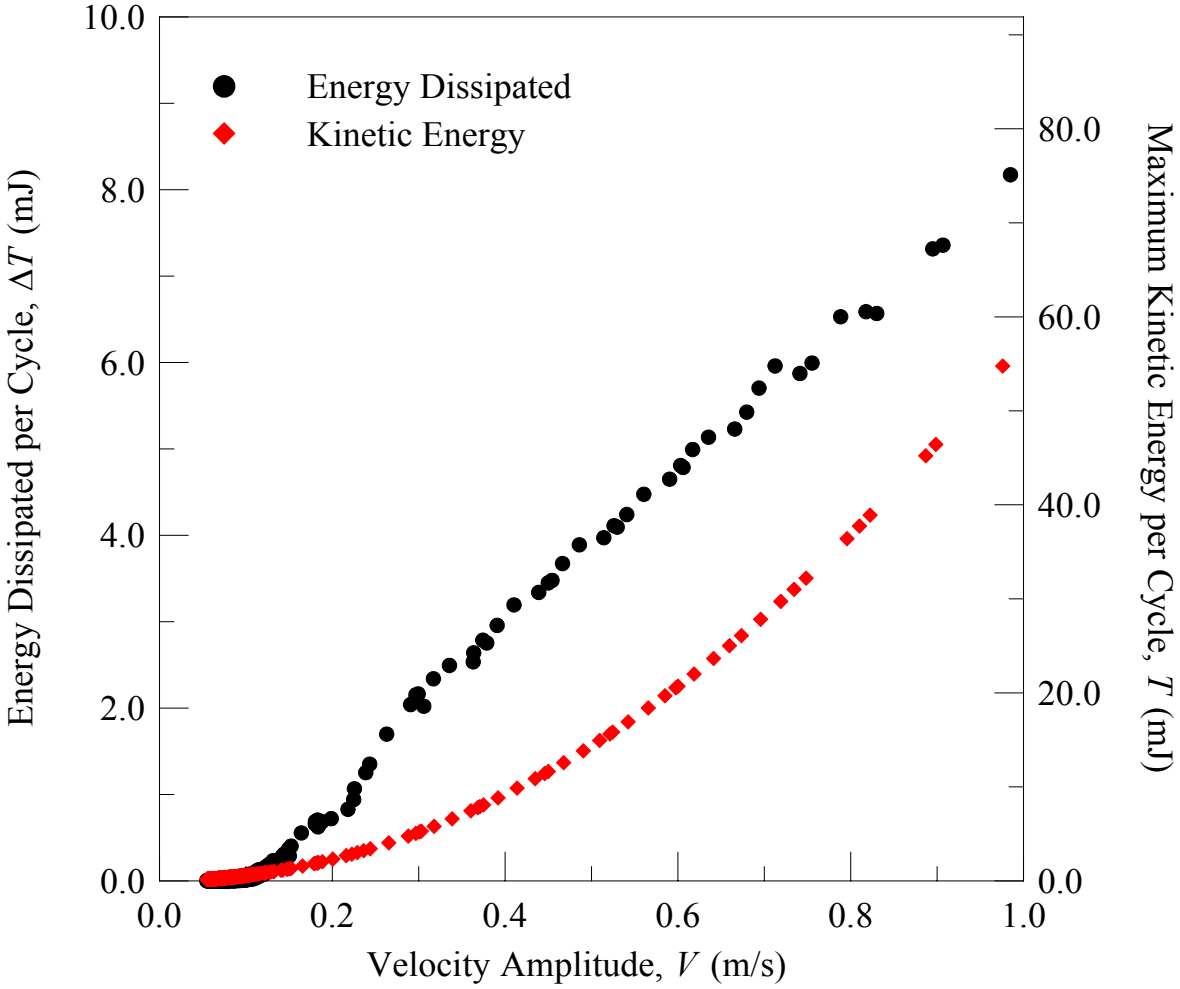

Figure 3. Kinetic energy dissipated per cycle versus velocity amplitude. 1.2 mm lead spheres, $\mu = 0.1$ and $\Delta = 5.65$.

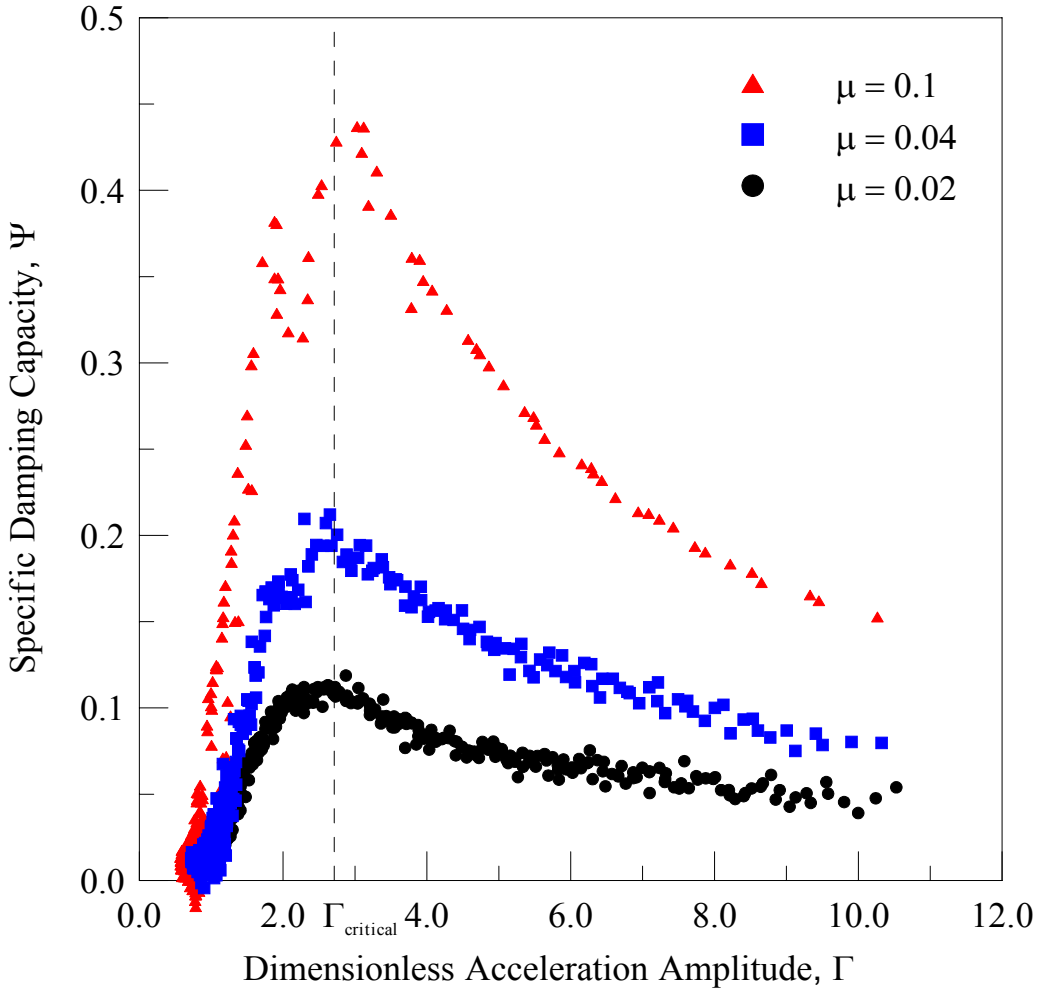

Figure 4. Specific damping capacity of beam with particles versus dimensionless acceleration amplitude. 1.2 mm lead spheres and $\Delta = 5.65$.

4.2 The Effects of Particle Materials on Damping

While keeping the mass ratio constant at $\mu = 0.06$, PID was measured for different value of Δ. The particles tested and their properties are given in Table 1.

Table 1. Particles tested, for $\mu = 0.06$

Particle Material	Diameter (mm)	Density (g/cm^3)	Approximate Number of Particles
Glass Spheres	1.12	2.50	2,800
Steel Spheres	1.17	7.84	900
Lead Spheres	1.20	11.3	620
Tungsten Carbide Pellets	~0.50	13.0	7,500

Figures 5 (a) to 5 (f) present the experimental results. Within the uncertainty of measurement (which is rather large), it is interesting to observe that Ψ is essentially independent of the material of the particles.

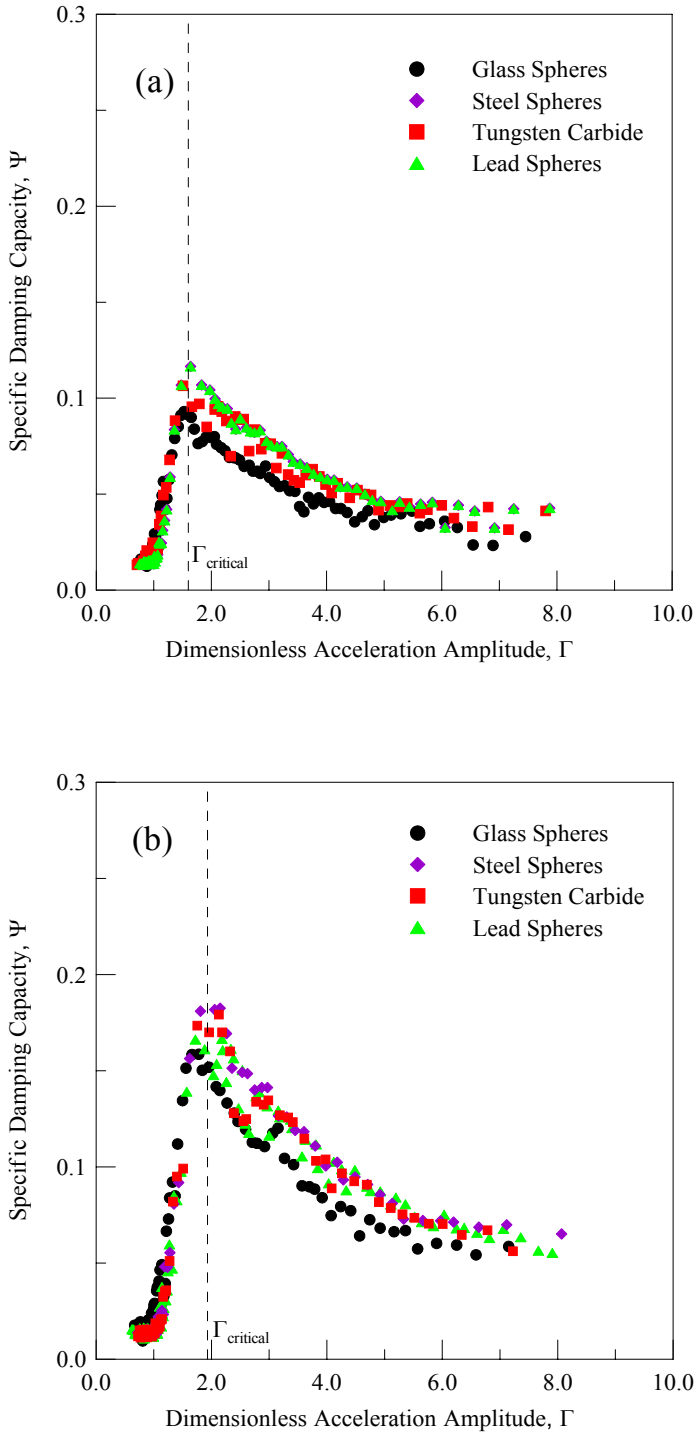

Figure 5. Comparison of different particle materials for the same mass ratio. $\mu = 0.06$ (a) $\Delta = 1.13$; (b) $\Delta = 2.26$;

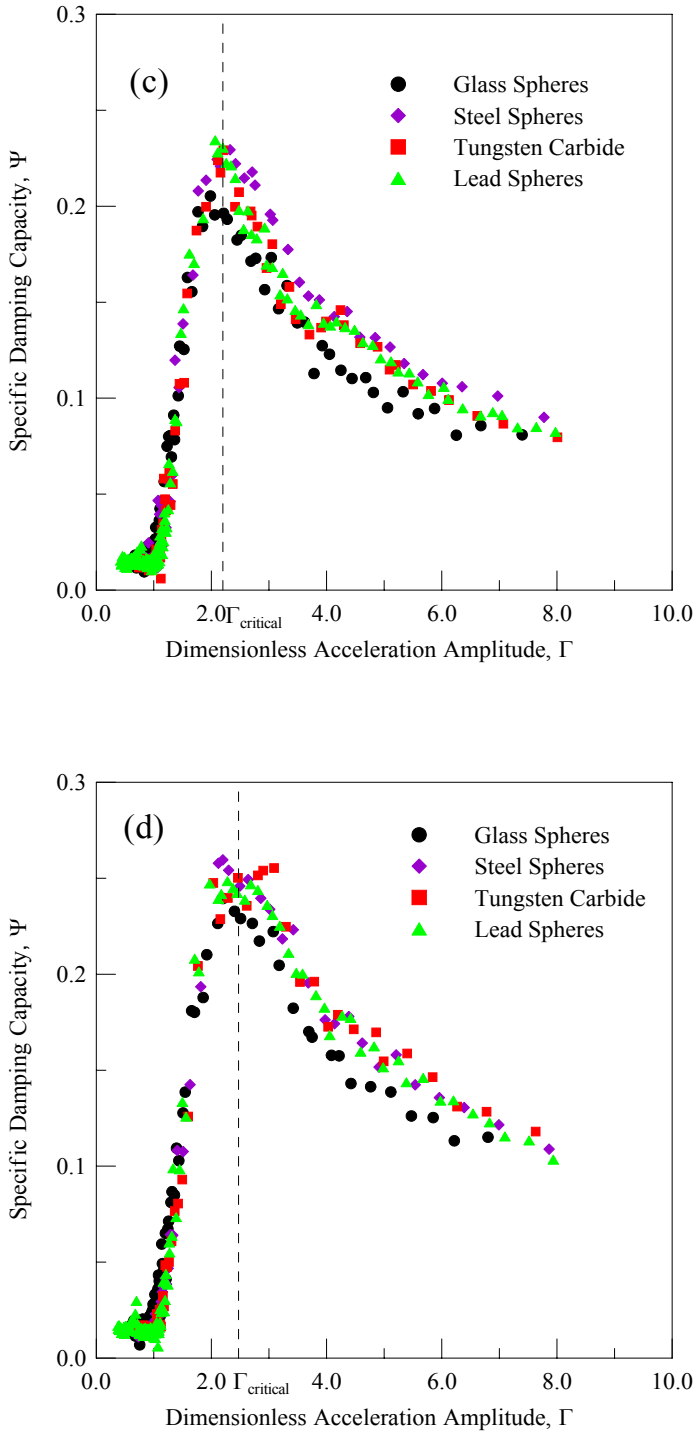

Figure 5. (continued) (c) $\Delta = 3.36$; (d) $\Delta = 4.52$;

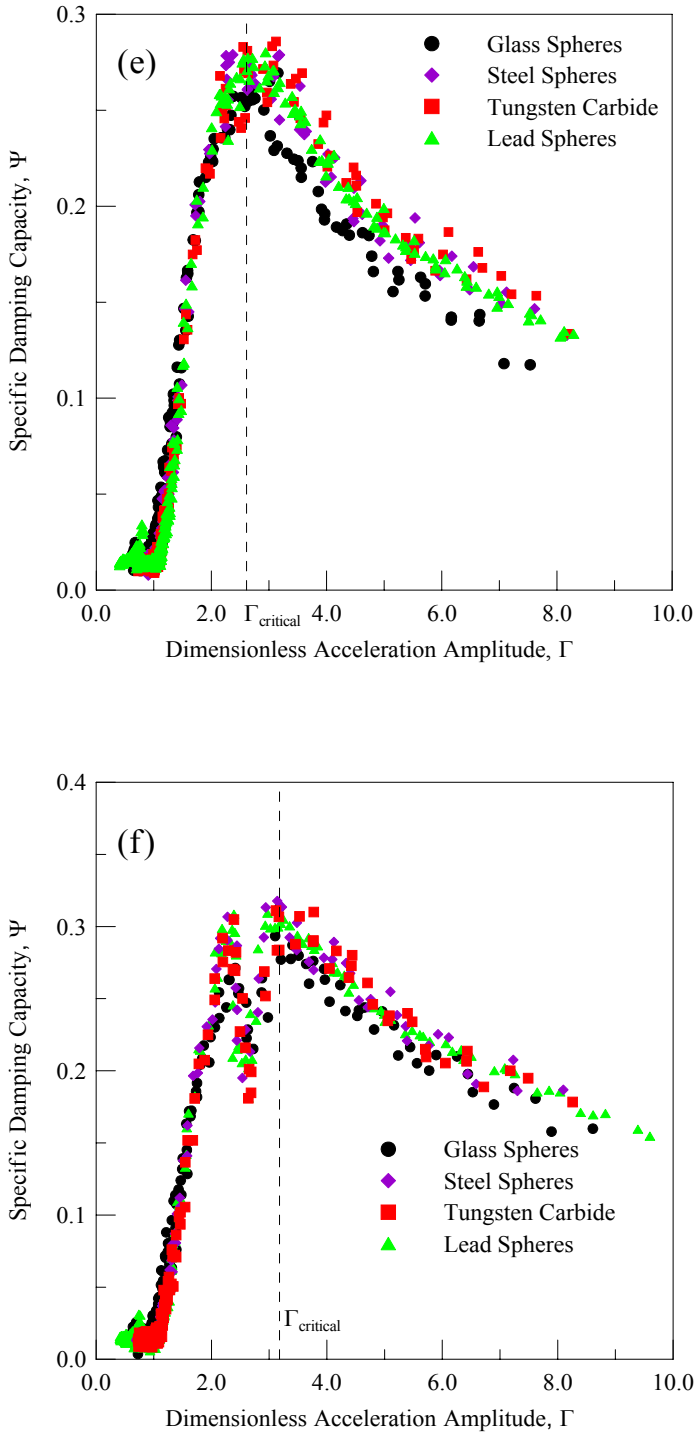

Figure 5. (continued) (e) $\Delta = 5.25$; (f) $\Delta = 7.91$.

4.3 The Effects of Number of Particles

We also performed experiments in which we controlled the number of particles used. The particles used were 1.12 mm glass spheres, 1.17 mm steel spheres, and 1.2 mm lead spheres. Tests were conducted for 1, 2, and 5 layers of particles at $\Delta = 5.65$. One layer contains 207 particles that fully cover the floor of the enclosure. For glass, steel, and lead spheres one layer of particles corresponds to a mass ratio of 0.004, 0.013, and 0.02 respectively. Comparison will be made for different particle materials at the same layer. Since for the same layer each particle material has different mass, the damping needs to be mass normalized.

From equation (1) and (7), specific damping capacity depends on mass ratio by a factor of $\mu/(1+\mu)^2$. Then, the damping can be mass normalized by the factor, and we define $\Psi_m = \Psi(1+\mu)^2/\mu$ as the mass normalized damping. Mass normalizing the damping of all particles tested produces interesting results as presented in Figures 6 (a) until 6 (c). The results for 1 layer glass spheres are not presented because the scatter in the data becomes large after mass normalization (division by a small number). For 1 layer of particles, the difference in Ψ_m is noticeable. For 5 layers, Ψ_m becomes the same for all particle types. Hence, we may actually observe that particle impact damping is independent of particle material at sufficiently large number of particles.

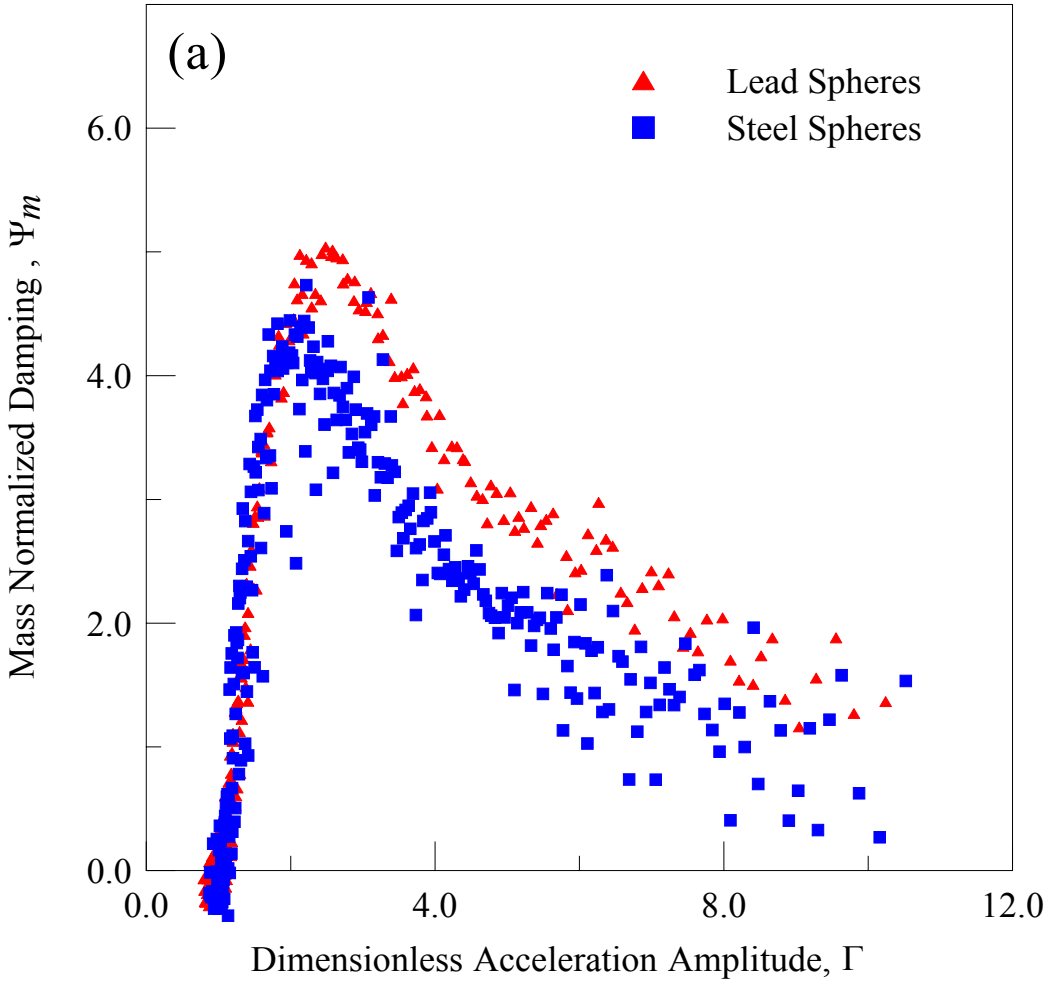

Figure 6. Comparison of different materials for the same size, shape, and number of particles. $\Delta = 5.65$. (a) 1 layer. 207 Particles;

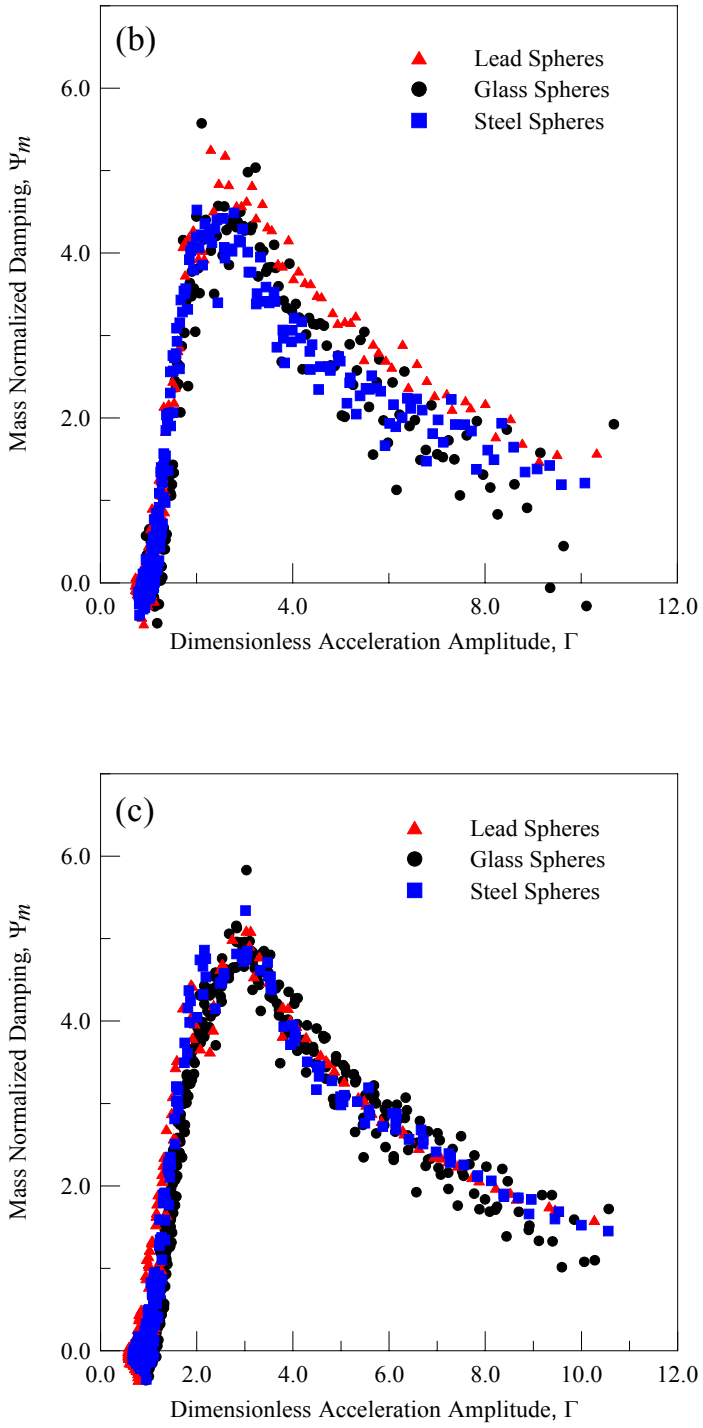

Figure 6. (continued) (b) 2 layers. 414 particles; (c) 5 layers. 1035 particles.

4.4 The Effects of Particle Size

A set of tests was also conducted to investigate the effects of particle size for the same particle material and mass ratio. With glass spheres, three different sizes were tested. The diameters of the spheres were 3 mm, 1.12 mm, and 0.5 mm. Tests were conducted for $\mu = 0.02$ and $\Delta = 5.65$. Since the mass ratio was constant, the number of particles would vary. For each particle size this corresponds to 50, 1035, and 11,000 particles respectively. The results are presented in Figure 7. For 3 mm glass spheres, the damping is noticeably lower than that of the other sphere sizes. Damping is essentially the same for the smaller particles.

In order to investigate the behavior of particle impact damping at sufficiently large number of particles, we doubled the number of 3 mm glass spheres tested at the same Δ. The damping was then compared again with the original damping of 0.5 mm and 1.12 mm glass spheres after mass normalization. The results are presented in Figure 8. As shown in the figure, the mass normalized damping was the same for all particles tested. For that reason, it is more appropriate to think that the way size of the particles affects damping is related to the number of particles the enclosure can hold.

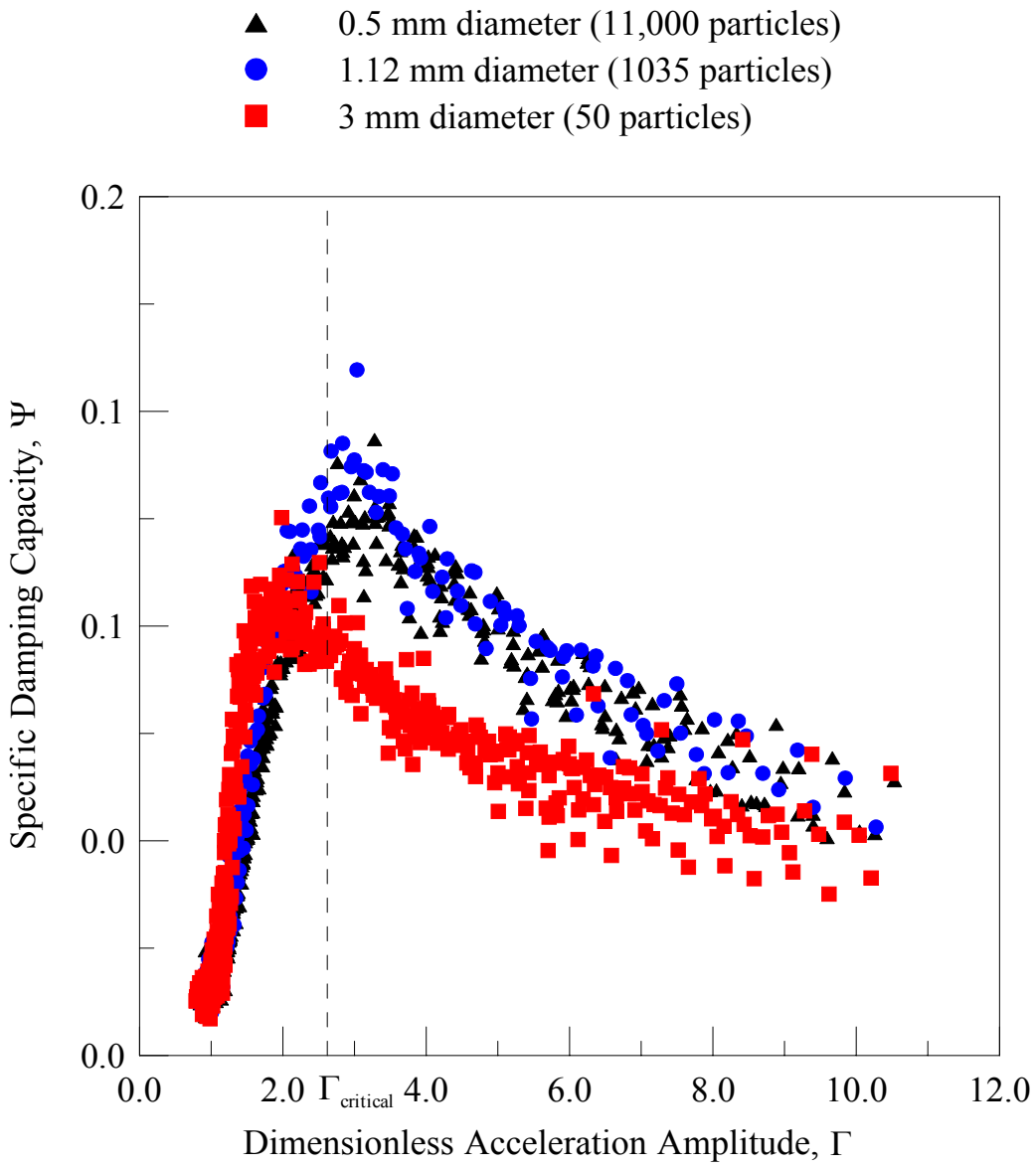

Figure 7. Comparison of different particle sizes for the same mass ratio. Glass spheres. $\mu = 0.02$. $\Delta = 5.65$.

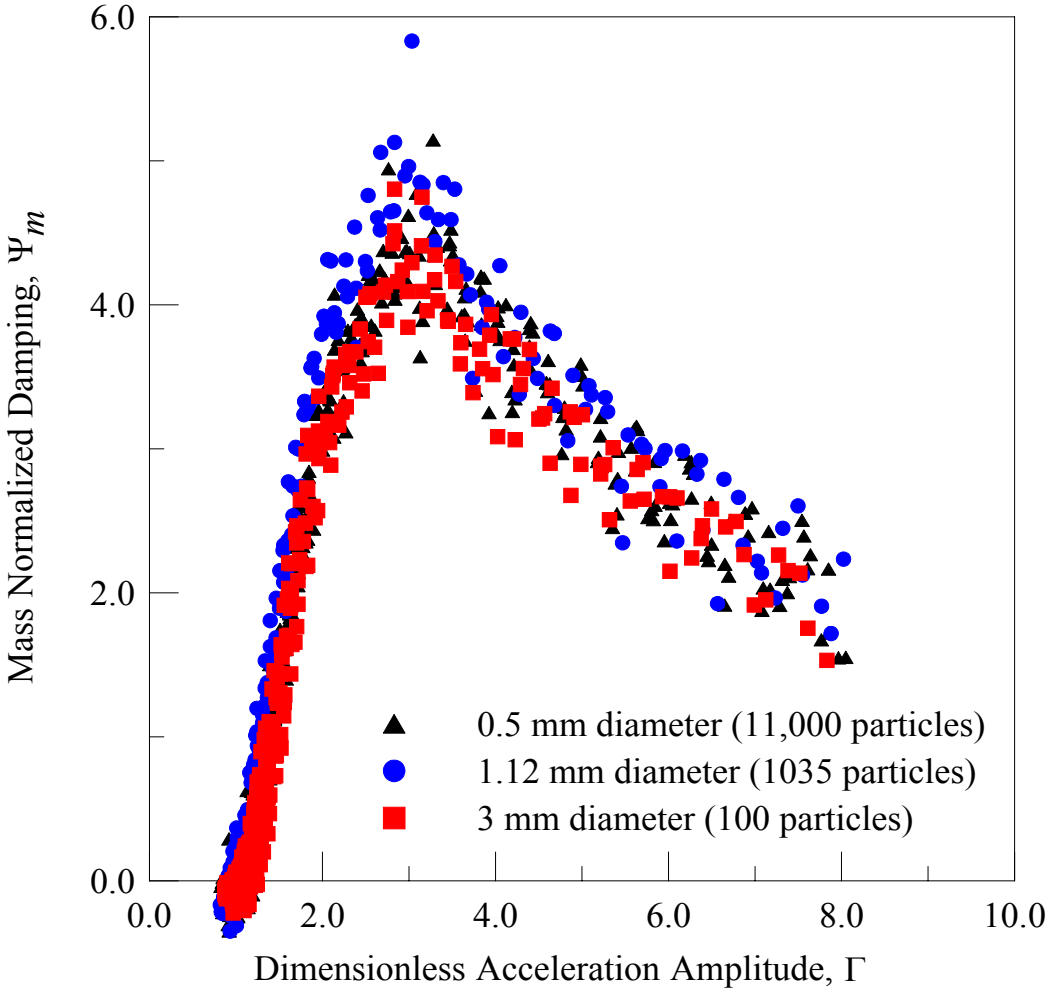

Figure 8. Comparison of different particle sizes and number of particles. Glass spheres. $\Delta = 5.65$.

4.5 Dust Like Particles

In order to collect more experimental data, tests were conducted with particles of more various shapes, smaller sizes, and significantly higher number of particles at the same mass. The particles tested were sand, lead dust, and steel dust with irregular shape. Particle impact damping could be a very versatile damping technique if the results from these tests show similar observation (i.e. PID is insensitive to particle material at sufficiently large number of particles).

All tests were conducted with $\mu = 0.06$ and $\Delta = 5.25$. The particles tested and their properties are given in Table 2. The results are presented in Figure 9.

Table 2. Dust like particles tested, for $\mu = 0.06$

Particle Material	Average Equivalent Diameter (mm)	Density (g/cm^3)	Approximate Number of Particles
Sand	0.2	1.70	900,000
Steel Dust	0.5	7.84	13,000
Lead Dust	0.2	11.3	140,000

As shown in the figure, damping of each particle material is remarkably different. Damping of lead dust reaches a maximum of 25% at $\Gamma = 2.6$, steel dust reaches a maximum of 17% at $\Gamma = 4$, and sand reaches a maximum of 13% at $\Gamma = 4.5$. These differences may be due to the difference in material properties of each particle that govern the energy dissipation mechanism. In fact, damping increases as material density of the particles increases. There could be more factors other than material properties that cause the difference in damping, such as how the particles travel during vibration,

whether as a lumped mass or as a cloud which is more likely in reality. Further study is needed to determine more accurately how energy is dissipated during the experiments.

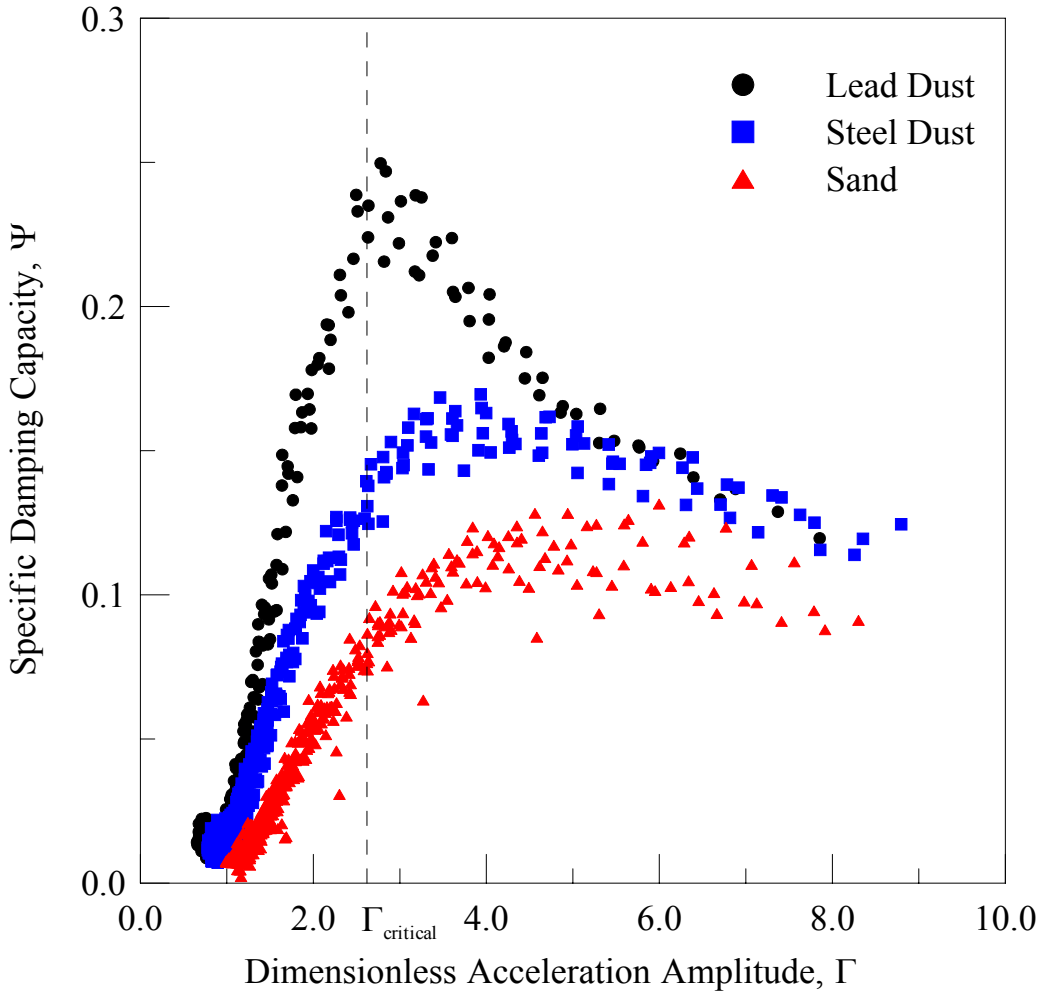

Figure 9. Experimental results of dust like particles. $\mu = 0.06$. $\Delta = 5.25$.

5. CONCLUSION

Experiments were conducted to collect damping characteristic of various particle materials and sizes. Although many phenomena of particle impact damping observed in the experiments still do not have satisfactory explanation yet, the experimental data collected here is offered as a damping database for future development of an analytical model of particle impact damping.

This research pushed the boundaries of the normal use of the laser vibrometer in an effort to make new discoveries. We learned valuable lessons such as the frequency limitations of the laser and its capability in measuring transient vibrations. We also learned that utilizing a cantilever beam in transient vibration to measure particle impact damping might not be the best method. For future study, it appears that particle impact damping should be measured in forced, rather than free, vibration in order to obtain more accurate results.

REFERENCES

1. C. Saluena, T. Poschel, and S. E. Esipov 1999 *Physical Review* **59**(4), 4422-4425. Dissipative properties of vibrated granular materials.

2. Chen Tianning, Mao Kuanmin, Huang Xieqing, and Michael Yu Wang 2001 *Proceedings of SPIE on Smart Structures and Materials* **4331**, 294-301. Dissipative mechanisms of non-obstructive particle damping using discrete element method.

3. A. Papalou and S.F Masri 1996 *Earthquake Engineering and Structural Dynamics* **25**(3), 253-267. Response of impact dampers with granular materials under random excitation.

4. C. Cempel and G. Lotz 1993 *Journal of Structural Engineering* **119**(9), 2624-2652. Efficiency of vibrational energy dissipation by moving shot.

5. N. Popplewell and S. E. Semergicil 1989 *Journal of Sound and Vibration* **133**(2), 193-233. Performance of the bean bag impact damper for a sinusoidal external force.

6. H. V. Panossian 1991 *Machinery Dynamics and Element Vibrations* ASME DE-Vol. 36, 17-20. Nonobstructive particle damping (NOPD) performance under compaction forces.

7. H. V. Panossian 1992 *Journal of Vibration and Acoustics* **114**, 101-15. Structural damping enhancement via non-obstructive particle impact damping technique.

8. R. D. Friend and V. K. Kinra 2000 *Journal of Sound and Vibration* **233**(1), 93-118. Particle impact damping.

VITA

Kun Saptohartyadi Marhadi
c/o Marhadi
Exploration CPI Rumbai
Pekanbaru, Riau 28271
Indonesia

Master of Science in Aerospace Engineering, December 2003
Texas A&M University, College Station, Texas

Bachelor of Science in Aerospace Engineering, May 2000
Texas A&M University, College Station, Texas